

Performance study of the TOP counter with the 2 GeV/c positron beam at LEPS

K. Matsuoka*, For the Belle II PID group

KMI, Nagoya University

E-mail: matsuoka@hepl.phys.nagoya-u.ac.jp

The TOP (Time-Of-Propagation) counter is a novel ring-imaging Cherenkov detector for particle identification in the Belle II experiment. It mainly consists of a 2.7 m long quartz radiator bar and 32 micro-channel-plate photomultiplier tubes (MCP-PMTs). It measures the time of propagation of the Cherenkov photons in the quartz bar with a resolution of 50 ps to reconstruct the Cherenkov “ring” image in the detection time and position plane. A prototype TOP counter which was close to the final design was tested with a 2 GeV/c positron beam at LEPS (Laser Electron Photon facility at SPring-8). We obtained a beautiful pattern of the Cherenkov image and understood the quartz optics and the MCP-PMT performance well. We also succeeded in reconstructing the speed of the positron event-by-event as expected.

*Technology and Instrumentation in Particle Physics 2014,
2-6 June, 2014
Amsterdam, the Netherlands*

*Speaker.

1. Introduction

The TOP (Time-Of-Propagation) counter [1–6] is a novel ring imaging Cherenkov detector for particle identification (PID) in the Belle II experiment [7]. It aims to identify up to 3 GeV/c kaons and pions with a pion efficiency of 95% and a fake-pion rate of 5% or better.

The TOP counter mainly consists of a $260 \times 45 \times 2$ cm³ quartz radiator bar, a 10 cm long quartz prism, a spherical mirror (6.5 m in radius of curvature) and two rows of 16 micro-channel-plate photomultiplier tubes (MCP-PMTs) [8–12] as shown in Fig. 1. It is a compact and nonmassive detector, which is suitable for the collider experiment.

Cherenkov photons generated in the quartz bar by a charged particle propagate in the bar as they are totally reflected on the boundaries between the quartz and the air. The path of the Cherenkov photons to the MCP-PMTs, or the time of propagation, depends on the Cherenkov angle or the speed of the charged particle. By measuring the time of propagation of the Cherenkov photons as well as the time of flight of the charged particle for about 1 m in addition to the momentum, position and angle of the charged particle measured by the inner trackers, the TOP counter identifies the mass of the charged particle. The number of Cherenkov photons detected by the MCP-PMTs is about 20 per particle. To achieve the aimed PID performance it is essential for the TOP counter to propagate the Cherenkov image undistorted without photon loss, to detect the photons with a high efficiency and to measure the time of propagation of each photon with a time resolution better than 50 ps.

The quartz components and the MCP-PMT were developed in success. Their performance is described in this paper. A prototype TOP counter was assembled and its performance was evaluated with a 2 GeV/c positron beam at LEPS (Laser Electron Photon facility at SPring-8) [13]. The results of the beam test are also discussed.

2. TOP counter components

2.1 Quartz bar

The Cherenkov photons reach the MCP-PMTs after an order of 100 reflections on the quartz bar surfaces. To maintain the Cherenkov image on the reflections the quartz bar surfaces have to be flat and in parallel with the facing surface. To minimize the loss of the Cherenkov photons

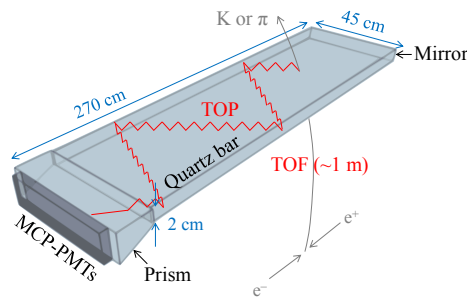


Figure 1: Schematic view of the TOP counter. An example of a charged particle (kaon or pion) trajectory and one path of the Cherenkov light in the quartz is indicated in this figure.

Length	1250 ± 0.50 mm
Width	450 ± 0.15 mm
Thickness	20 ± 0.10 mm
Flatness	$< 6.3 \mu\text{m}$
Parallelism	< 4 arcsec
Roughness	$< 5 \text{ \AA}$ (RMS)

Table 1: Part of the quartz bar specifications. The flatness, parallelism and roughness are for the largest surfaces.

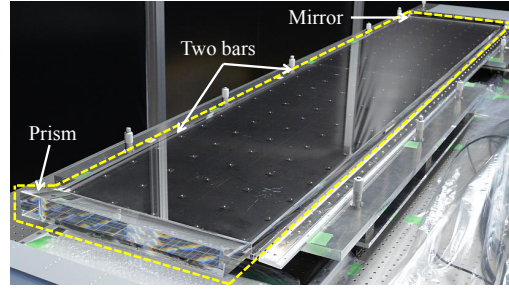


Figure 2: Photograph of the glued quartz bars, mirror and prism of the prototype TOP counter. The quartz component is indicated with the dashed line.

the surfaces have to be smooth. Thus the specifications of the quartz bar are determined as listed in Table 1. Less than $6.3 \mu\text{m}$ flatness and less than 4 arcsec parallelism are required to keep displacement of the Cherenkov photon at the MCP-PMT within the position resolution of the MCP-PMT. Less than 5 \AA (RMS) roughness is required to keep loss of the Cherenkov photons at the reflections before reaching the MCP-PMT less than 20%. Because it is difficult to polish a long quartz bar, two 125 cm long bars are polished separately by companies and then are glued together with optical adhesive of high transmittance. On the both ends of the 250 cm long bar a 10 cm long quartz bar whose spherical end is coated with the aluminum mirror and a 10 cm long quartz prism are also glued. The spherical shape of the mirror is meant to reduce the chromatic error of the Cherenkov light [14].

For the prototype TOP counter, all the quartz components were glued together successfully as shown in Fig. 2. The dimensions are the same as the final ones except the length of the bar and the mirror radius of curvature. The length of the prototype is shorter by 61 mm and the radius is 5.0 m. The internal surface reflectance and bulk transmittance of the quartz bars were measured to be greater than 99.90% and greater than 98.5%/m, respectively. They satisfy our requirements.

2.2 MCP-PMT

The MCP-PMT for the TOP counter was developed at Nagoya University in collaboration with HAMAMATSU Photonics K.K. To cover the end face of the prism with a small dead region, it is $27.6 \times 27.6 \text{ mm}^2$ square in shape. The photocathode size is $23 \times 23 \text{ mm}^2$ and the anode size is $22 \times 22 \text{ mm}^2$. The anode is divided by 4×4 . The photocathode is made of NaKSbCs. The quantum efficiency (QE) as a function of the wavelength is shown in Fig. 3. The maximum QE is typically 28% around 360 nm wavelength. The MCP-PMT contains two $400 \mu\text{m}$ thick MCPs to have enough gain (greater than 5×10^5 in 1.5 T) for single photon detection. The diameter and the bias angle of the micro channel of the MCP are $10 \mu\text{m}$ and 13 degrees, respectively. The aperture ratio of the MCP is about 60%. Because the photoelectron is multiplied in these thin MCPs, the MCP-PMT has a small transit time spread (TTS) less than 40 ps. Figure 4 shows a distribution of the hit timing for single photons from a pico-second pulse laser measured by a CAMAC TDC. The TTS is defined by the standard deviation of the Gaussian fitted to the peak of the distribution. The tail on the right side of the peak corresponds to events where the photoelectron bounces on the first MCP surface [15].

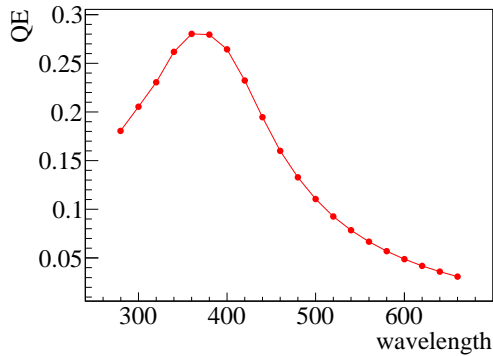


Figure 3: Typical QE of the MCP-PMT as a function of the wavelength.

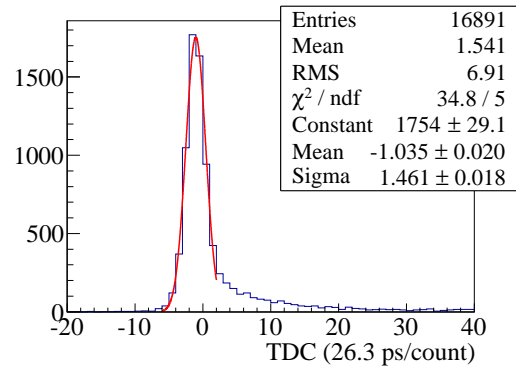


Figure 4: Hit timing distribution of the MCP-PMT for single photons. A Gaussian is fitted to the peak of the distribution.

2.3 Readout electronics

A multi-gigasample per second waveform sampling ASIC, called IRS, developed at Hawaii University is used for the front-end readout electronics of the TOP counter. Figure 5 (left) shows a prototype of the front-end module used for the beam test. It consisted of an array of the IRS3B ASICs controlled by FPGAs. The digitized waveforms were sent via a fiber-optic cable to the back-end which was composed of a COPPER/FINESSE data acquisition system [16, 17]. The prototype TOP counter was equipped with full 32 MCP-PMTs and the four front-end modules. The total number of MCP-PMT anode channels was 512 though 90 channels were not read out in the beam test due to some problems.

Another readout electronics shown in Fig. 5 (right) was also used in the beam test. The front-end module consisted of four constant fraction discriminator (CFD) boards where the MCP-PMT signal was amplified and digitized to a differential ECL (Emitter-Coupled Logic) signal. The ECL signal was sent via a twisted pair cable to a VME TDC, CAEN V1290A. The TDC has a timing

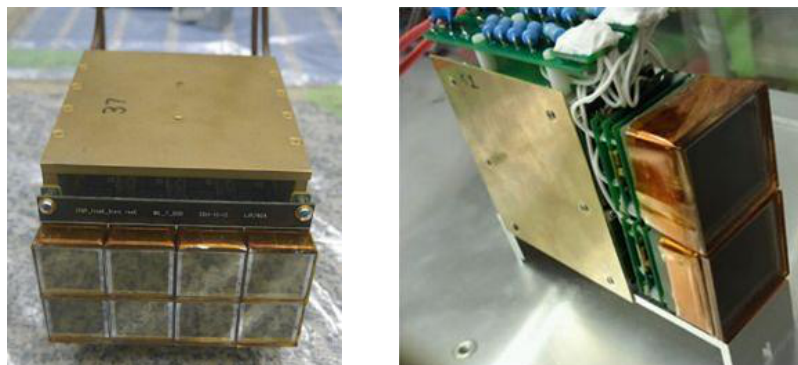


Figure 5: Photographs of the IRS3B front-end module with eight MCP-PMTs (left) and the CFD front-end module with two MCP-PMTs (right).

resolution of about 20 ps after a dedicated calibration. The timing resolution of the CFD readout system was tested with a test pulse. It was consistent with the TDC resolution. To reduce the number of readout channels, the 16 outputs of each MCP-PMT were merged into four at the MCP-PMT socket. Therefore the number of readout channels of the prototype TOP counter was 128 in case of the CFD readout.

3. Performance study of the TOP counter

To study the performance of the TOP counter, the prototype TOP counter was tested with the 2 GeV/c positron beam at LEPS. Two different data sets were taken with the IRS3B and CFD readout systems.

3.1 Setup of the beam test

At the LEPS beam line a high energy photon beam (less than 2.4 GeV) is available. It is produced by the backward Compton scattering of 355 nm laser photons on the 8 GeV electron beam in the SPring-8 synchrotron. The setup of the beam test is shown in Fig. 6. The photon beam impinging on a 1.5 mm thick Pb target to create electron and positron pairs. The momentum of the pairs was measured by the LEPS spectrometer; a dipole magnet operated at 0.7 T, three drift chambers (DC1, DC2 and DC3) and a wall of TOF counters. To trigger on 2 GeV/c positrons, two pairs of $40 \times 40 \text{ mm}^2$ and $5 \times 5 \text{ mm}^2$ scintillation trigger counters were put between DC3 and the TOF counters. The distance between the pairs was about 1 m. The TOP counter was put between the trigger counters so that the beam incident angle was normal to the quartz bar. The beam hit position was about 135 cm away from the MCP-PMT array. The trigger was issued at the coincidence of the four trigger counters and the trigger rate was about 10 Hz. The hit position and angle on the quartz bar was monitored by two pairs of vertical and horizontal scintillating fiber trackers. Each tracker consisted of double layers of five scintillating fibers whose diameter and interval were 2 mm and 2.2 mm, respectively. The fluctuation of the beam angle measured by the trackers was about 1.8 mrad. To eliminate electromagnetic shower events, the number of hit TOF counters was required to be one. The beam timing (t_0) was obtained from the accelerator RF

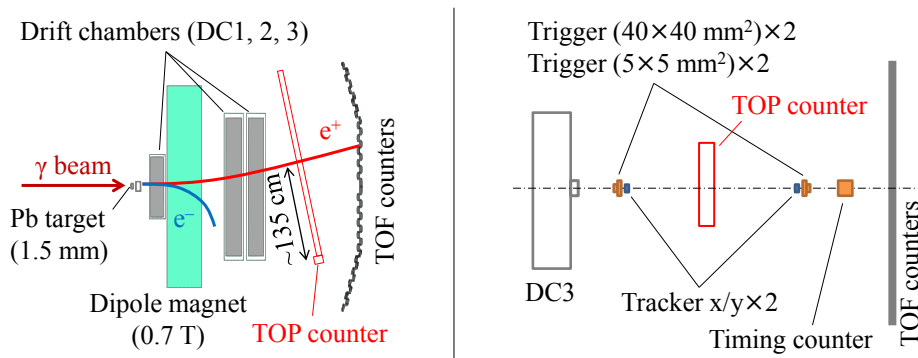


Figure 6: Setup of the beam test at LEPS. (Left) Top view of the LEPS spectrometer. (Right) Side view of the beam test setup.

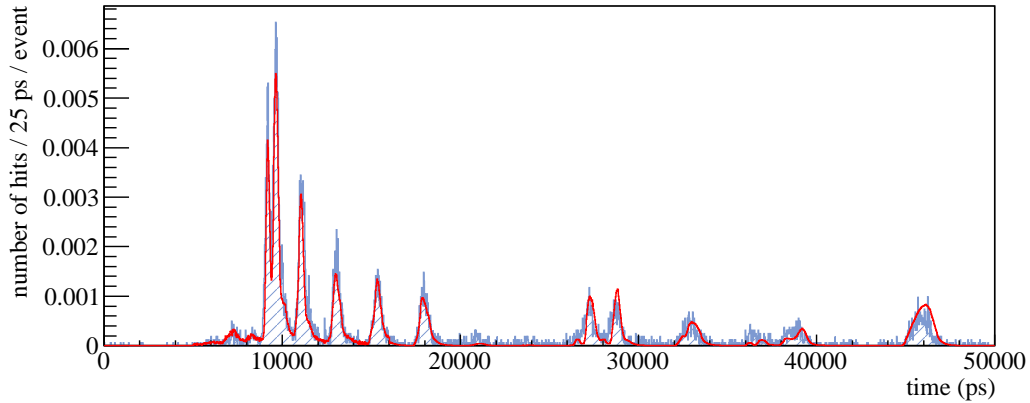


Figure 7: Accumulated distribution of the MCP-PMT hit timing for a center channel measured by the CFD readout (hatched histogram). The PDF (line) is overlaid.

signal. The t_0 resolution was measured to be about 30 ps using a Cherenkov timing counter which consisted of a quartz block and an MCP-PMT.

3.2 Results of the beam test

The MCP-PMT hit timing relative to t_0 was recorded for each channel. Figure 7 shows the accumulated distribution of the hit timing for a channel at the center of the MCP-PMT array measured by the CFD readout. The earliest peak around 9.2 ns corresponds to the Cherenkov photons which are generated in the direction toward the MCP-PMT and reach the channel via the shortest path. The Cherenkov photons generated in the other directions are reflected on the sides of the quartz bar and make the following peaks. Those reflected on the mirror appear after 26 ns. The component earlier than the first peak originates from electromagnetic showers. In this figure the probability density function (PDF) calculated analytically is overlaid and it agrees well with the data. The height of each peak depends on the quartz surface reflectance and transmittance, the QE of the MCP-PMT and the QE dependence on the photon incident angle and polarization [12]. The width of each peak is determined mainly by the chromatic dispersion of the Cherenkov light and the TTS of the MCP-PMT. The tail on the right side of each peak is made by the bounce of the photoelectron on the first MCP surface as shown in Fig. 4 and a cross-talk of the MCP-PMT signal to the adjacent channels. Therefore the agreement of the height, width and tail of each peak means that the quartz optics and the performance of the MCP-PMT are well understood.

Figure 8 shows the two-dimensional accumulated hit distribution measured by the IRS3B readout and the expected one by a Monte Carlo simulation (MC) based on the Geant4 simulation toolkit [18, 19]. The pattern of the Cherenkov image matches between the data and MC. In the data, differences of the time origin among the channels due to the electronics were corrected using the hit timing for a pulse laser which was irradiated to the MCP-PMTs through the quartz bar.

The number of hits per event distributed as shown in Fig. 9. The mean number of hits is 32.0 for the CFD data and 32.6 for the MC. This agreement also supports our understanding of the quartz optics and the photon detection efficiency of the MCP-PMT and the CFD electronics. The

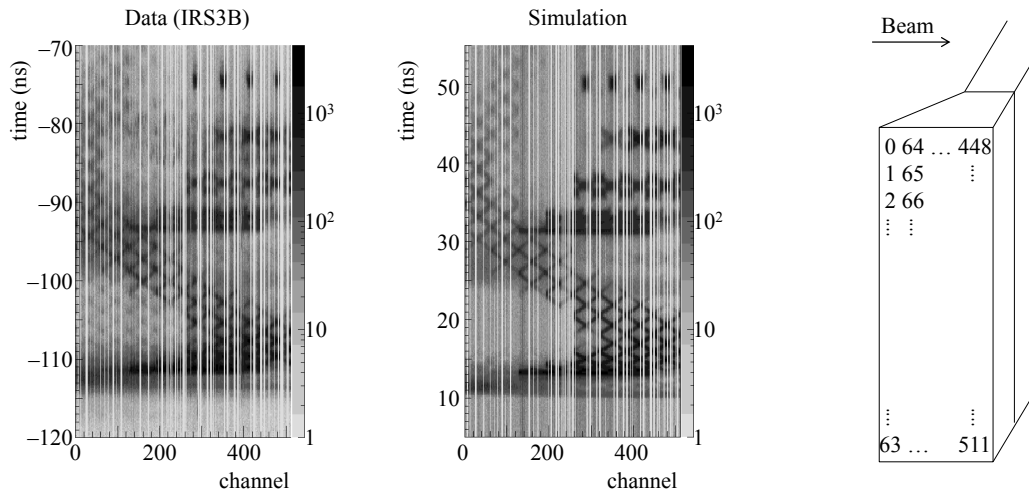


Figure 8: Accumulated hit distribution measured by the IRS3B readout (left) and the expectation by the MC (center). The vertical blank bands correspond to the dead channels. The channel number is assigned as shown in the right figure, which is a schematic view of the prism end.

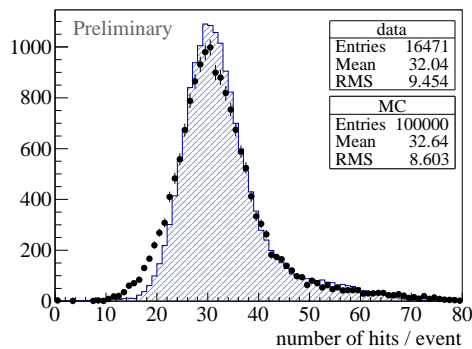


Figure 9: Number of hits per event measured by the CFD readout. The hatched histogram is the estimation by the MC. It is normalized to the number of data events.

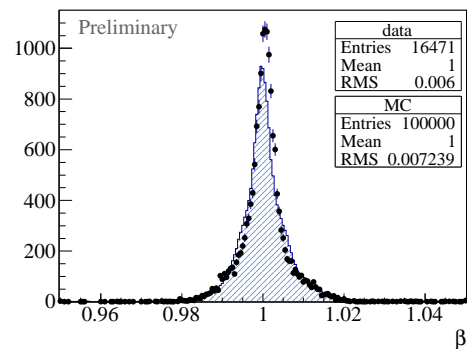


Figure 10: Reconstructed β from the CFD data. The hatched histogram represents the reconstructed β for the MC. It is normalized to the number of data events.

MC also well represents the electromagnetic shower background, which appears in the tail on the right side of the number of hits distribution.

For the two-dimensional measurements of the hit timing and channel taken by the CFD readout, the speed of the incident positron relative to the one of light in vacuum (β) was reconstructed event-by-event with a maximum likelihood method. For the 2 GeV/c positron β equals 1.0000. The distribution of the reconstructed β is shown in Fig. 10. The mean and RMS of the distribution are 1.0005 and 0.0060, respectively. They are nearly consistent with the MC, where the mean is 1.0004 and the RMS is 0.0072. The slight discrepancy of the distributions is under investigation.

4. Conclusions

The TOP counter is a novel ring imaging Cherenkov detector for particle identification in Belle II. The main components of the TOP counter, the quartz bar and the MCP-PMT, were developed in success. Their performance was confirmed by testing the prototype TOP counter with the 2 GeV/c positron beam at LEPS. The performance of the TOP counter was evaluated by reconstructing β of the positron event-by-event; the mean and RMS of the β distribution was 1.0005 and 0.0060, respectively, which were nearly consistent with the expectation by the MC.

Acknowledgments

This work was supported by MEXT Grant-in-Aid for Scientific Research on Innovative Areas “Elucidation of New Hadrons with a Variety of Flavors”. We acknowledge assistance of the LEPS collaboration to the beam test.

References

- [1] M. Akatsu, et al., *Nucl. Instr. and Meth. A* **440** (2000) 124.
- [2] T. Oshima, *ICFA Instrumentation Bulletin* **20** (2000) 2.
- [3] T. Oshima, *Nucl. Instr. and Meth. A* **453** (2000) 331.
- [4] Y. Enari, et al., *Nucl. Instr. and Meth. A* **494** (2002) 430.
- [5] Y. Enari, et al., *Nucl. Instr. and Meth. A* **547** (2005) 490.
- [6] K. Matsuoka, For the Belle II PID Group, *Nucl. Instr. and Meth. A* **732** (2013) 357.
- [7] T. Abe, et al., KEK-REPORT-2010-1, 2010.
- [8] M. Akatsu, et al., *Nucl. Instr. and Meth. A* **528** (2004) 763.
- [9] K. Inami, et al., *Nucl. Instr. and Meth. A* **592** (2008) 247.
- [10] N. Kishimoto, et al., *Nucl. Instr. and Meth. A* **564** (2006) 204.
- [11] T. Jinno, et al., *Nucl. Instr. and Meth. A* **629** (2011) 111.
- [12] K. Matsuoka (For the Belle II PID group), *Nucl. Instr. and Meth. A* (2014), <http://dx.doi.org/10.1016/j.nima.2014.05.003>.
- [13] T. Nakano, et al., *Nucl. Phys. A* **64** (2001) 71.
- [14] Y. Arita, *Phys. Procedia* **37** (2012) 621.
- [15] C. Field, et al., *Nucl. Instr. and Meth. A* **553** (2005) 96.
- [16] Y. Igarashi, et al., *eConf* **C0303241** (2003) TUGP009.
- [17] T. Higuchi, et al., *eConf* **C0303241** (2003) TUGT004.
- [18] S. Agostinelli, et al., *Nucl. Instr. and Meth. A* **506** (2003) 250.
- [19] J. Allison, et al., *IEEE Trans. Nucl. Sci.* **53** (2006) 270.